# High-energy and high-peak-power Q-switched $Er^{3+}/Dy^{3+}$ codoped fluoride fiber oscillator aiming at the 2.94 μm water absorption peak

**Xiangyu Zhao (赵翔宇), Hongyu Luo (罗鸿禹)*，Jianfeng Li (李剑峰), Yong Liu (刘永)**

State Key Laboratory of Electronic Thin Films and Integrated Devices, School of Optoelectronic Science and Engineering, University of Electronic Science and Technology of China, Chengdu 611731, China

*Corresponding author: hongyuluo@uestc.edu.cn

Received Month X, XXXX; accepted Month X, XXXX; posted online Month X, XXXX

In this Letter, we demonstrate high-energy and high-peak-power nanosecond pulse generation aiming at the 2.94 μm water absorption peak, from a 980 nm diode-clad-pumped actively Q-switched $Er^{3+}/Dy^{3+}$ codoped fluoride fiber oscillator, for the first time. Operating at the 2943 nm wavelength locked by a diffraction grating in a Littrow configuration, stable Q-switching with the shortest temporal width of 41 ns has been obtained at a low repetition rate of 100 Hz. The maximum pulse energy of 108 μJ and peak power of 2.48 kW are primarily limited by the thermal damage of the bare fluoride fiber facet for pump coupling, and represent the records of pulsed fiber oscillators around 2.94 μm, to the best of our knowledge. This advanced nanosecond laser source provides an optional promising tool for laser medical applications.

***Keywords**: high energy; high peak power; Q-switching; fluoride fiber; water absorption.*
*DOI: 10.3788/COLXXXXXX.XXXXXX.*

## 1. Introduction

Coherent laser sources emitting around 3 μm are always attracting continuous attention in biomedical applications, because of strong absorption experienced in liquid water. Currently, this kind of lasers have been extensively applied in skin[1,2] and endodontic[3] treatments, lithotripsy[4], ophthalmology[5], etc. To compliment the great successes achieved by solid-state lasers such as $Er^{3+}$:YAG laser[6,7], the laser architecture based on advanced fluoride fibers with compact arrangement, excellent beam quality, and maintenance-free design, provides us another alternative[8-12]. As the pioneer of this class of lasers, $Er^{3+}$-doped fluoride fiber lasers operating on the $^4I_{11/2}\rightarrow{}^4I_{13/2}$ transition have showed outstanding performance at ~2.8 μm, recording the highest continuous wave (CW) power of 42 W[9] and slope efficiency of up to ~60%[13]. Based on this transition, pulse generation with μs~fs scale temporal widths based on the techniques of Q-switching[14], gain-switching[15], and mode-locking[16] has been also reported. Wherein, nanosecond pulses with high energies and peak powers are particularly favored in laser surgery because of reduced thermal effects unwanted. To realize this kind of pulses, Q-switching, especially based on actively switched scheme implemented by externally controlled modulators such as acousto-optic modulator (AOM)[17], electro-optic modulator [18] or even mechanical chopper wheel[19], is a popular route because of its unique behavior for energy storage before releasing a pulse, albeit at the sacrifice of some average power. Until now, the maximum pulse energy of 560 μJ (53 ns width)[20] and peak power of 16 kW (13 ns width)[18] (not simultaneously) have been acquired from actively Q-switched $Er^{3+}$-doped fluoride fiber oscillators. Following fiber amplifiers, the pulse energy could be even scaled to 0.75 mJ with a width of 95 ns and an estimated peak power of 7.4 kW[21]. Nevertheless, it remains challenging when the wavelength was pushed towards 2.94 μm, the strongest water absorption peak which has an absorption coefficient of 3 times higher than at 2.8 μm. Despite the availability of efficient CW lasing at 2.94 μm using a long fiber needed for compensating the long-wavelength gain[22], the resulting high gain, however, easily leads to the premature onset of lasing, therefore impeding the achieving of high energy and peak power. Accordingly, most actively Q-switched reports on $Er^{3+}$-doped systems were around or below 2.8 μm[17-20,23]. As its neighbor in spectral domain, the $^5I_6\rightarrow{}^5I_7$ transition of $Ho^{3+}$ is faced with the similar trouble, although it has a slightly red-shifted emission spectrum. The four-level nature particularly in a fiber architecture results in easy prelasing even in the low Q factor phase of Q-switching. As a result, the maximum pulse energy and peak power at 2.95 μm reported were 4.16 μJ and 12.5 W, respectively[24]. At the shorter wavelength of 2.87 μm, the pulse energy and peak power were only enhanced to 19 μJ and 576 W, respectively[25], indicating the contradictory requirements for obtaining high pulse energy and peak power, and the wavelength close to 2.94 μm. As a contrast, the three- or quasi-three-level $Dy^{3+}$ ($^6H_{13/2}\rightarrow{}^6H_{15/2}$) not only can operate around 2.94 μm in a short fiber (helpful for narrowing pulse thereby enhancing peak power), but also requires a large population inversion fraction for lasing (beneficial for energy storage hence scaling energy). Recently, Pajewski et al. employed an AOM to Q-switch an 1.1 μm core-pumped $Dy^{3+}$-doped fluoride fiber oscillator at 2.912 μm yielding a pulse width of 74 ns[26], whereas only a low pulse energy of 17 μJ and peak power of 201 W were obtained due to the resonant pump excited state absorption (ESA) that depopulated the laser upper state[27], detrimental for energy storage. From this view, clad pumping maybe more suggested due to weaker pump intensity, however, this will lead to significantly increased laser threshold[28]. To address the issue, 980 nm[29,30] and 660 nm[31] clad-pumped $Er^{3+}/Dy^{3+}$ codoped fluoride fiber oscillators have been developed recently where $Er^{3+}$ aims to absorb the pump and then transfers energy to $Dy^{3+}$ for emission, thus circumventing the potential pump ESA of $Dy^{3+}$. Based on this platform, we presented active Q-switching in the

region of 2.9~3.6 μm very recently[32]. In that case, to demonstrate the wideband potential, 660 nm diode was adopted to activate both the ~3 μm band of $Dy^{3+}$ and ~3.5 μm band of $Er^{3+}$, while a moderate fiber length was selected to balance their gains for maximizing the spectral tuning range. Accordingly, the pulse energy and peak power at 2.951 μm were only 24 μJ and 55 W, respectively, with a pulse width of 404 ns[32]. If focusing on the $Dy^{3+}$ emission around 2.94 μm, 980 nm pumping should be a more efficient way owing to smaller quantum defect[30].

In this work, we employ a commercially available 980 nm diode as the pump, demonstrating an AOM actively Q-switched $Er^{3+}/Dy^{3+}$ codoped fluoride fiber oscillator with a short pulse width of 41 ns, in which a diffraction grating has been used to lock the wavelength at 2.943 μm. The significantly enhanced pulse energy of 108 μJ and peak power of 2.48 kW, far beyond our recent presentation[32], set the new records for pulsed fiber oscillators around 2.94 μm.

## 2. Experiments

### 2.1 Setup

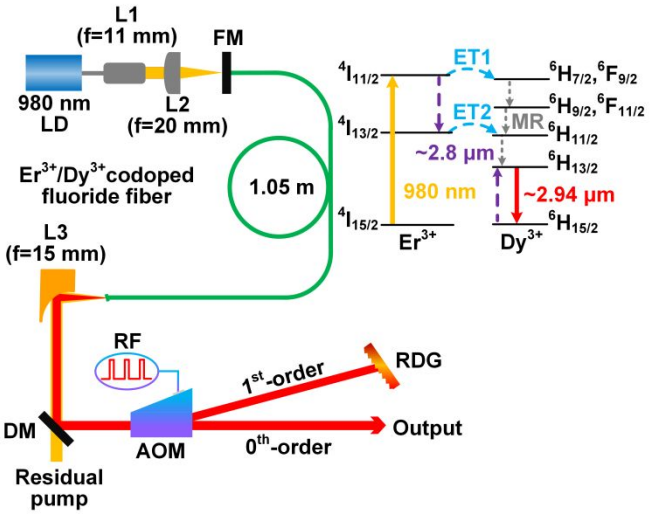


Fig. 1. Schematic setup of the actively Q-switched $Er^{3+}/Dy^{3+}$ codoped fluoride fiber oscillator diode-pumped at 980 nm. LD, laser diode; L1, collimator; L2, aspheric lens; FM, front mirror; L3, off-axis parabolic reflector; DM, dichroic mirror; RF, radio frequency; RDG, ruled diffraction grating. Inset: simplified energy level diagram with some relevant transitions (ET, energy transfer; MR, multiphonon relaxation).

The setup of the actively Q-switched $Er^{3+}/Dy^{3+}$ codoped fluoride fiber oscillator is depicted in Fig. 1, where pumping is provided by a commercial multimode LD (BWT, China) pigtailed to a silica fiber with a core diameter of 105 μm and a numerical aperture (NA) of 0.15. The gain fiber provided by *FiberLabs Inc.*, is a segment of 4/0.25 mol.% $Er^{3+}/Dy^{3+}$ codoped double-clad fluoride fiber. The fiber core has a diameter of 18.8 μm and a NA of 0.13. The clad has a circular diameter of 249 μm and a NA of 0.5, with an absorption coefficient of 1~2 dB/m at 980 nm (provided by the manufacturer). In this case, the short fiber length of 1.05 m was selected in order to extract more energy (i.e., higher pulse energy) by increasing the prelasing threshold, and achieve a shorter pulse width thus a higher peak power, at the sacrifice of the pump absorption ratio (i.e.,~30% measured). The fiber facet close to the pump was perpendicularly cleaved and butted against the FM (highly transmissive at 980 nm but reflective at 2.7 ~3.7 μm at 0°) as the cavity feedback, while the other one was 8° angle-cleaved to inhibit prelasing. The pump was coupled into the fiber clad via a pair of lenses (i.e., L1 and L2) with an estimated efficiency of 86%. The outputs from the angle-cleaved facet were collimated using the L3 before being incident on the DM (highly transmissive at 980 nm but reflective at 2.7~3.7 μm at 45°) to remove the residual pump, and then steered into a Ge AOM with Bragg angle. The AOM, anti-reflective coated at 2.5~5 μm, has a maximum diffraction efficiency of 80% and a rise time of ≤140 ns/mm, and was driven by a 68 MHz RF source modulated by a rectangular wave from a function generator with variable duty cycle. The 0th-order light functions as the output, and 1st-order diffraction is resonant by a reflector, ensuring no feedback left due to incomplete diffraction of the AOM when the lasing is held off, hence inhibiting prelasing[25]. Here the reflector is a narrow-band RDG (Thorlabs, GR2550-30035) in a Littrow configuration, aiming to suppress the undesirable amplified spontaneous emission (ASE) components at the laser wavelength, therefore leading to a shorter pulse width thus a higher peak power[18,19], while locking the wavelength for stable Q-switching. The total cavity length of 2.25 m containing a long free-space distance of 1.2 m (ensuring narrow filtering bandwidth), corresponds to a cavity round trip time of 18 ns. The inset plots the simplified energy level diagram with some relevant transitions, where the $^6H_{13/2} \rightarrow {}^6H_{15/2}$ transition can be activated by pumping at 980 nm, based on the processes of ET1, ET2, and ~2.8 μm emission and absorption.

The laser power was measured using a high-resolution thermal sensor with a detectable power of 100 μW-5 W (Thorlabs, S405C). The pulse signals were recorded using a HgCdTe detector with a ≤3 ns time constant (VIGO, PCI-2TE-12) connecting with a 500 MHz oscilloscope. The optical spectra were collected by a spectrometer (Yokogawa, AQ6377) with a minimum resolution of 0.2 nm. Note that the above measurements were performed after a long-pass filter (>2.9 μm) except the spectrum.

### 2.2 Results

First, we rotated the RGD to search for the position which could lock the wavelength at 2.94 μm while aligning the AOM slightly to maximize the output power. In our experiment, the maximum launched pump power was set at 24.9 W for reducing the thermal damage risk of the bare fluoride fiber facet for pump coupling, where its temperature was up to 80°C identified by a thermal imager.

Then, the laser performance variations with the repetition rate from 100 Hz to 6 kHz have been recorded as displayed in Fig. 2, where the duty cycle was adjusted at the same time to maintain stable Q-switching. One can observe that the pulse energy increases rapidly with the decreased repetition rate from 6 kHz to 1 kHz as a result of longer time used for energy storage, and then tends to be saturated below ~1 kHz, corresponding to the scale of inverse upper-state lifetime of 650 μs. In addition, a higher

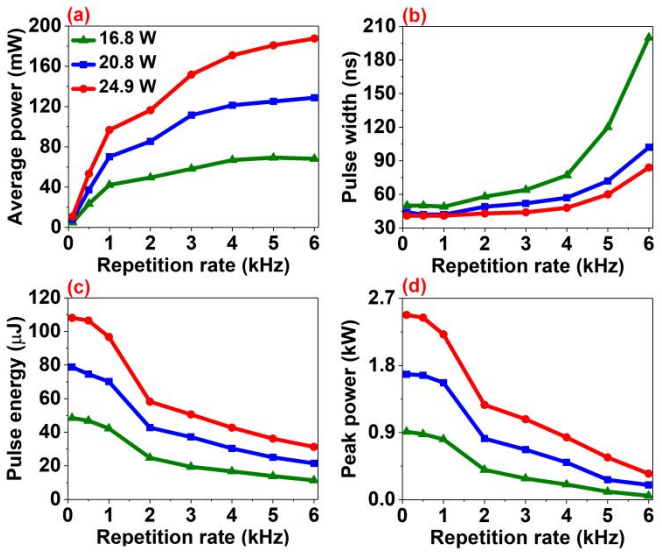


Fig. 2. (a) Average power, (b) pulse width, (c) pulse energy, and (d) peak power versus repetition rate at different launched pump powers.

pump power yields a higher pulse energy without any saturation signs, implying the possibility of energy scaling. On contrary, the pulse width decreases sharply firstly with the decreased repetition rate owing to the fact that the increased pulse energy leads to a stronger temporal modulation of the net gain, and thus a faster rise and decay of the optical power. Then it exhibits a saturation behavior as a result of the saturated pulse energy, where a higher pump power results in the earlier saturation relative to the repetition rate, similar to the previously reported actively Q-switched $Dy^{3+}$-doped fluoride fiber oscillators[26,32,33]. With the increase of the repetition rate, the average power increases and then approaches a constant value, approximately equal to the output power under the CW condition[33]. In terms of the peak power, its evolution behavior is similar to the pulse energy as a result of the relatively moderate variation of the pulse width.

To clearly reveal the dependence of the output performance on the launched pump power, the case at the low repetition rate of 100 Hz has been exhibited as shown in Fig. 3. The average power increases almost linearly with the launched pump power, where the low slope efficiency was mainly caused by the use of short fiber and large energy loss via fluorescence at such a low repetition rate.

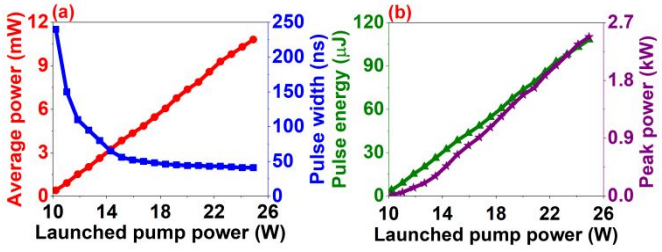


Fig. 3. (a) Average power and pulse width, and (b) pulse energy and peak power versus launched pump power at the repetition rate of 100 Hz.

Of note is that the outputs include many linearly polarized components, showing a polarization extinction ratio (PER) of ~10 dB since both the AOM and RDG are polarization sensitive. If replacing the RDG with a broadband reflector, the PER would decrease to 6~7 dB. To further improve the PER, a polarizer (e.g., Brewster window, film polarizer, and Glan laser prism) with the orientation parallel to the mounting base of the AOM (ensuring a large diffraction efficiency) can be introduced into the cavity between the DM and AOM. The pulse width deceases and then tends to be saturated resulting from Q-switching dynamics. At the launched pump power of 24.9 W, the shortest pulse width of 41 ns (2~3 times the cavity round trip time) was obtained, which is, to our knowledge, the shortest of Q-switched and gain-switched fiber oscillators beyond 2.9 μm. By shortening the cavity length (either fiber or free-space length) under the premise of ensuring sufficient gain and narrow filtering bandwidth, while increasing the modulation depth of the Q-switching element (i.e., AOM diffraction efficiency in this case), a shorter pulse width is expected. Owing to the fixed repetition rate, the pulse energy exhibits a same linear evolution behavior as the average power, thus leading to an almost linear evolution for the peak power apart from the initial stage. At the maximum pump power, the record pulse energy of 108 μJ and peak power of 2.48 kW (calculated based on a shape factor of 0.94 for Gaussian pulses) have been achieved, which are more than 4 times[32] and one order of magnitude[26] higher than the previous best results from either Q-switched or gain-switched fiber oscillators around 2.94 μm (defined within 2.9~3 μm), respectively. Further scaling of the pulse energy and peak power was primarily limited the pump power allowed by the bare fiber facet for pump coupling. To solve this issue, a potential way is to splice the LD pigtail with the $Er^{3+}/Dy^{3+}$ codoped fluoride fiber, in which a high-reflectivity fiber Bragg grating at the laser wavelength is directly written to replace the FM as the feedback. To significantly scale the output level, the use of a master oscillator power amplifier scheme is an optional solution. Figure 4 shows the corresponding pulse train and single pulse waveform with a basically Gaussian shape, where no evident temporal interference fringes are observed due mainly to the limited bandwidth of the

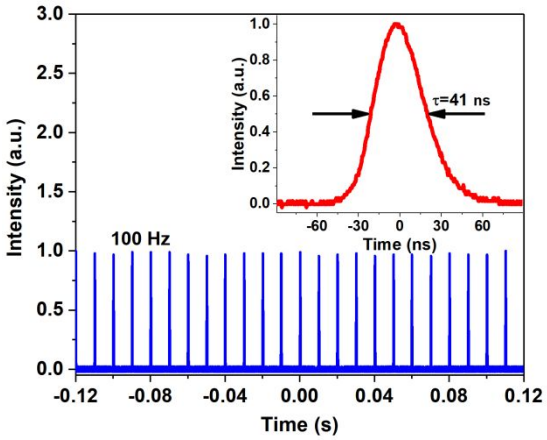


Fig. 4. Pulse train and single pulse waveform (inset) at the repetition rate of 100 Hz at the launched pump power of 24.9 W.

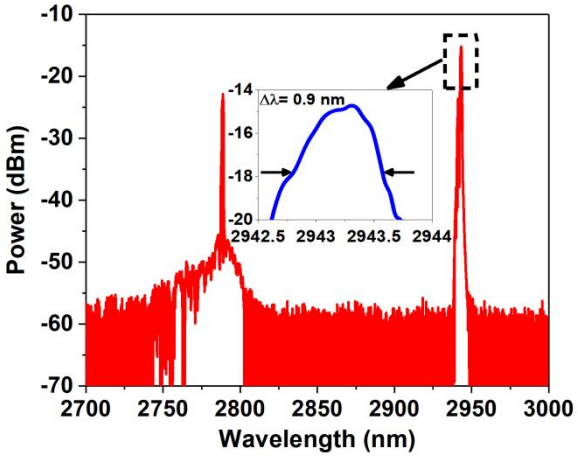


Fig. 5. Optical spectrum at the repetition rate of 100 Hz at the launched pump power of 24.9 W. Inset: zoomed optical spectrum.

detector, although the pulse wavelength was shifted twice by the AOM per round trip. The low amplitude fluctuation of 2% indicates great stability.

At this pump power, the optical spectrum scanning from 2.7 μm to 3.1 μm was also recorded as plotted in Fig. 5, where the long-pass filter was removed in order to exhibit emission feature of the whole system. The strong laser signal centered at 2943 nm with a 3 dB bandwidth of 0.9 nm has been observed, where there are no obvious ASE components from the $^6H_{13/2}\rightarrow{}^6H_{15/2}$ transition of $Dy^{3+}$, indicating the filtering effect of the RDG. In the spectral blue region, however, the strong parasitic lasing at ~2.8 μm sitting on an obvious ASE pedestal from the $^4I_{11/2}\rightarrow{}^4I_{13/2}$ transition of $Er^{3+}$ was captured. This is not surprising in such a short fiber considering the high gain for the $Er^{3+}$ transition and weakened absorption of $Dy^{3+}$ at ~2.8 μm. Here, the actual power proportion of the ~2.8 μm emission was measured to be ~30%. To inhibit the unwanted ~2.8 μm components, appropriately increasing the $Dy^{3+}$ doping concentration to enhance the absorption is an alternative strategy. In addition, we found that with the repetition rate increasing from 100 Hz to 1 kHz, this power proportion significantly decreased to ~7% due to the enhanced absorption by $Dy^{3+}$ as a result of more ions returning to the $^6H_{15/2}$ state. Of note is that the ~2.8 μm signal was CW instead of pulses identified by the detector, because it was not resonant in the cavity closed by the FM and RDG. Nevertheless, it didn't impact the stability and energy scaling of the Q-switched pulses. Furthermore, the calculated normalized frequency of 2.61 at this wavelength, slightly higher than the cut-off frequency of 2.405, implies the quasi-single-mode operation of the pulses with a high brightness, although the quantitative characterization needs a beam quality analyzer which was absent in our lab. Based on an 1:1 imaging system, the optical fluence was estimated (according to the single-mode approximation) to be 36 J/cm$^2$, which has reached the levels required by skin treatment targeting shallow stratum corneum and epidermal layer (typical fluence of 2~20 J/cm$^2$ at ~2.94 μm[1,2,34]) and deeper tissue ablation with an improved demand of 25~100 J/cm$^2$[2,35-37]. Of note is that even at a higher repetition rate of 1 kHz which may be more preferred in some special medical applications[38,39], our fluence still could reach 31 J/cm$^2$ (estimated according to the value in Fig. 2(c)). These results highlight great medical potential of our source.

## 3. Conclusion

In this work, we report active Q-switching operation of a 980 nm diode-clad-pumped $Er^{3+}/Dy^{3+}$ codoped fluoride fiber oscillator towards the 2.94 μm water absorption peak. Based on a short fiber length of 1.05 m and a RDG for locking the wavelength, the stable nanosecond pulses with the shortest temporal width of 41 ns have been gotten at a low repetition rate of 100 Hz and the quasi-single-mode state. The achieved maximum pulse energy of 108 μJ and peak power of 2.48 kW, only limited by the damage risk of the bare fluoride fiber facet used for pump coupling, represent the highest levels of fluoride fiber oscillators around 2.94 μm (see Table 1), to the best of our knowledge. This high-performance nanosecond laser source provides a new opportunity for laser medical applications.

**Table 1. Representative Fluoride Fiber Oscillators Operating around 2.94 μm (Defined within 2.9~3 μm)**

| Pump wavelength [nm] | Dopant ions | Method[a] | Laser wavelength [nm] | Pulse width [ns] | Pulse Energy [μJ] | Peak power [W] | Ref. |
|---|---|---|---|---|---|---|---|
| 980 | $Er^{3+}$ | CW | 2938 | / | / | 30.5 | [22] |
| 1150 | $Ho^{3+}/Pr^{3+}$ | CW | 2942 | / | / | 6.3 | [11] |
| 1690 | $Dy^{3+}$ | CW | 2962 | / | / | 1.6 | [40] |
| 1150 | $Ho^{3+}/Pr^{3+}$ | ML | 2940 | 0.027 | 0.0081 | 170 | [41] |
| 1150 | $Ho^{3+}$ | GS | 2920 | 283 | 5.4 | 17.9 | [42] |
| 1100 | $Dy^{3+}$ | GS | 2947 | 530 | 2.73 | 4.84 | [43] |
| 1150 | $Ho^{3+}$ | QS | 2949 | 331 | 4.16 | 12.5 | [24] |
| 1100 | $Dy^{3+}$ | QS | 2912 | 74<br>84.5 | 13.6<br>17 | 184<br>201 | [26] |
| 660 | $Er^{3+}/Dy^{3+}$ | QS | 2951 | 404 | 24 | 55 | [32] |
| **980** | **$Er^{3+}/Dy^{3+}$** | **QS** | **2943** | **41** | **108** | **2480** | **This work** |

[a]CW, continuous wave; ML, mode-locking; GS, gain-switching; QS, Q-switching.

## Acknowledgement

This work was supported by National Natural Science Foundation of China (NSFC) (62475035).

## References

1. E. F. Bernstein, J. F. Sanzo, J. Y. Wang, et al., "Low-fluence treatment with a novel fractionated 2910-nm fiber laser improves photodamage," Laser Surg. Med. 55, 35 (2023).
2. M. M. Selim, J. A. Lowery, H. S. Maredia, et al., "Clinical evaluation of a new fractional ablative 2910-nm erbium laser on photodamaged skin: A pilot study," Laser Surg. Med. 55, 715 (2023).
3. R. Guidotti, E. Merigo, C. Fornaini, et al., "Er:YAG 2940-nm laser fiber in endodontic treatment: a help in removing smear layer," Laser Med. Sci., 29, 69 (2014).
4. J. Qiu, J. Teichman, T. Wang, et al., "Comparison of fluoride and sapphire optical fibers for Er: YAG laser lithotripsy," J. Biophoton. 3, 277 (2010).
5. T. Klink, G. Schlunck, W. E. Lieb, et al., "Long-term results of Erbium YAG-laser-assisted deep sclerectomy," Eye 22, 370 (2008).
6. A. Zajac, M. Skorczakowski, J. Swiderski, et al., "Electrooptically Q-switched mid-infrared Er:YAG laser for medical applications," Opt. Exp. 12, 5125 (2004).
7. J. Yang, L. Wang, X. Wu, et al., "High peak power Q-switched Er:YAG laser with two polarizers and its ablation performance for hard dental tissues," Opt. Exp. 22, 15686 (2014).
8. F. Jobin, P. Paradis, Y. O. Aydin, et al., "Recent developments in lanthanide-doped mid-infrared fluoride fiber lasers [Invited]," Opt. Exp. 30, 8615 (2022).
9. Y. O. Aydin, V. Fortin, R. Vallée, et al., "Towards power scaling of 2.8 μm fiber lasers," Opt. Lett. 43, 4542 (2018).
10. M. R. Majewski and S. D. Jackson, "Highly efficient mid-infrared dysprosium fiber laser", Opt. Lett. 41, 2173 (2016).
11. S. Crawford, D. D. Hudson and S. D. Jackson, "High-power broadly tunable 3 μm fiber laser for the measurement of optical fiber loss," IEEE Photon. J. 7, 1 (2015).
12. S. Zhou，H. Luo，Y. Wang, et al., "Numerical design of an efficient $Ho^{3+}$-doped $InF_3$ fiber laser at ~3.2 μm," J. Electron. Sci. Technol. 22, 100261 (2024).
13. H. Luo, J. Shi. J. Chen, et al., "Towards high-power and -efficiency ~2.8 μm lasing: Lightly-erbium-doped $ZrF_4$ fiber laser pumped at ~1.7 μm," IEEE J. Lightw. Technol. 42, 316 (2024).
14. H. Luo, J. Li, J. Xie, et al., "High average power and energy microsecond pulse generation from an erbium-doped fluoride fiber MOPA system," Opt. Exp. 24, 29022 (2016).
15. P. Pascal, V. Fortin, Y. O. Aydin, et al., "10 W-level gain-switched all-fiber laser at 2.8 μm," Opt. Lett. 43, 3196 (2018).
16. S. Duval, M. Bernier, V. Fortin, et al., "Femtosecond fiber lasers reach the mid-infrared," Optica 2, 623 (2015).
17. S. Lukasz, L. Pajewski, S. Lamrini, et al., "High peak power Q-switched Er: ZBLAN fiber laser," IEEE J. Lightw. Technol. 39, 6572 (2021).
18. Y. Shen, Y. Wang, F. Zhu, et al., "200 μJ, 13 ns Er:ZBLAN mid-infrared fiber laser actively Q-switched by an electro-optic modulator," Opt. Lett. 46, 1141 (2021).
19. Y. Shen, Y. Wang, K. Luan, et al., "High peak power actively Q-switched mid-infrared fiber lasers at 3 μm," Appl. Phys. B 123, 1 (2017).
20. S. Lamrini, K. Scholle, M. Schäfer, et al., "High-energy Q-switched Er:ZBLAN fibre laser at 2.79 μm," Proc. Eur. Conf. Lasers Electro-Opt. Eur. Quantum Electron. Conf. CJ_7_2 (2015).
21. W. Du, Y. Bai, Y. Cui, et al., "Mid-IR pulse amplification to ~millijoule energies in a single transverse mode using large core Er: ZBLAN fibers operating at 2.8 μm," Opt. Exp. 30, 46170 (2022).
22. V. Fortin, M. Bernier, S. T. Bah, et al., "30 W fluoride glass all-fiber laser at 2.94 μm," Opt. Lett. 40, 2882 (2015).
23. S. Tokita, M. Murakami, S. Shimizu, et al., "12 W Q-switched Er:ZBLAN fiber laser at 2.8 μm," Opt. Lett. 36, 2812 (2011).
24. J. Li, Y. Yang, D. D. Hudson, et al., "A tunable Q-switched $Ho^{3+}$-doped fluoride fiber laser," Laser Phys. Lett. 10, 045107 (2013).
25. T. Hu, D. D. Hudson, and S. D. Jackson, "High peak power actively Q-switched $Ho^{3+}$,$Pr^{3+}$-co-doped fluoride fibre laser," IEEE Electron. Lett. 49, 766 (2013).
26. L. Pajewski, L. Sójka, S. Lamrini, et al., "Experimental investigation of actively Q-switched $Dy^{3+}$ doped fluoride single mode fiber laser operating near 3 μm," IEEE J. Lightw. Technol. 42, 809 (2024).
27. L. Sójka, L. Pajewski, M. Popenda, et al., "Experimental investigation of mid-infrared laser action from $Dy^{3+}$-doped fluorozirconate fiber," IEEE Photon. Technol. Lett. 30, 1083 (2018).
28. M. Z. Amin, M. R. Majewski, R. I. Woodward, et al., "Novel near-infrared pump wavelengths for dysprosium fiber lasers," IEEE J. Lightw.Technol. 38, 5801 (2020).
29. J. Wang, X. Zhu, R. A. Norwood, et al., "Beyond 3 μm $Dy^{3+}$/$Er^{3+}$ co-doped ZBLAN fiber lasers pumped by 976 nm laser diode," Appl. Phys. Lett. 118, 151101 (2021).
30. X. Zhao and H. Luo, "Efficient watt-level fluoride fiber laser beyond 3 μm enabled by direct diode pumping," Opt. Laser Technol. 181, 111715 (2024).
31. H. Luo, Y. Wang, J. Chen, et al., "Red-diode-clad-pumped $Er^{3+}$/$Dy^{3+}$ codoped $ZrF_4$ fiber: A promising mid-infrared laser platform," Opt. Lett. 47, 5313 (2022).
32. X. Zhao, H. Luo, J. Li, et al., "Tunable high energy pulse generation in the range of 2.9–3.6 μm enabled by an actively Q switched $Er^{3+}$/$Dy^{3+}$ codoped fluoride fiber oscillator," Opt. Lett. 49, 3721 (2024).
33. R. I. Woodward, M. Majewski, N. Macadam, et al., "Q-switched Dy:ZBLAN fiber lasers beyond 3 μm: Comparison of pulse generation using acousto-optic modulation and inkjet-printed black phosphorus," Opt. Exp. 27, 15032 (2019).
34. A. E. Ahmed, M. HamedKhater, and H. M. ALwafaey, "Role of fractional erbium YAG laser 2940 nm in treatment of eye wrinkles," Ann. Rom. Soc. Cell. Biol. 25, 19103 (2021).
35. T. Dumore and D. Fried, "Selective ablation of orthodontic composite by using sub-microsecond IR laser pulses with optical feedback," Laser Surg. Med. 27, 103 (2000).
36. K. Stock, R. Diebolder, F. Hausladen, et al., "Primary investigations on the potential of a novel diode pumped Er:YAG laser system for bone surgery," Proc. SPIE 8565, 756 (2013).
37. J. P. Rocca, M. Zhaoa, C. Fornaini, et al., "Effect of laser irradiation on aphthae pain management: a four different wavelengths comparison," J. Photoch. Photobio. B 189, 1 (2018).
38. D. Fried, R. Shori, and C. Duhn, "Backspallation due to ablative recoil generated during Q-switched Er:YAG abaltion of dental enamel," Proc. SPIE 3248, 78 (1998).
39. K. Stock, F. Hausladen, and R. Hibst, "Investigations on the potential of a novel diode pumped Er:YAG laser system for dental applications," Proc. SPIE 8208, 55 (2012).
40. Y. Wang, H. Luo, H. Gong, et al., "Watt-level and tunable operations of 3 μm-class dysprosium $ZrF_4$ fiber laser pumped at 1.69 μm," IEEE Photon. Technol. Lett. 34, 737 (2022).
41. M. Pawliszewska, M. R. Majewski, and S. D. Jackson, "Electronically tunable picosecond pulse generation from $Ho^{3+}$-doped fluoride fiber laser using frequency-shifted feedback," Opt. Lett. 45, 5808 (2020).
42. X. Zhang, W. Li, J. Li, et al., "Mid-infrared all-fiber gain-switched pulsed laser at 3 μm," Opto-Electron. Adv. 3, 190032 (2020).
43. H. Luo, Y. Xu, J. Li, et al., "Gain-switched dysprosium fiber laser tunable from 2.8 to 3.1 μm," Opt. Exp. 27, 27151 (2019).